CHEMISTRY
A EUROPEAN JOURNAL

Supporting Information

First Heterotrimetallic {3d-4d -4f} Single Chain Magnet, Constructed from Anisotropic High-spin Heterometallic Nodes and Paramagnetic Spacers

Diana Visinescu,[a] Augustin M. Madalan,[b] Marius Andruh,[b]* Carine Duhayon,[c,d] Jean-Pascal Sutter,[c,d]* Liviu Ungur,[e,f] Willem Van den Heuvel,[e] Liviu F. Chibotaru[e,f]

[a] *Coordination and Supramolecular Chemistry Laboratory Institute of Physical Chemistry "Ilie Murgulescu", Romanian Academy, Splaiul Independentei 202, Bucharest-060021 (Romania)*

[b] *Inorganic Chemistry Laboratory, Faculty of Chemistry, University of Bucharest, Str. Dumbrava Rosie nr. 23, Bucharest-020464 (Romania), Fax: (+) 4021-3159249, E-mail: marius.andruh@dnt.ro*

[c] *CNRS; LCC (Laboratoire de Chimie de Coordination), route de Narbonne, F-31077 Toulouse (France)*

[d] *Université de Toulouse, UPS, INPT ; LCC ; F-31077 Toulouse (France), Fax: (+) 33 5 61 55 30 03, E-mail: sutter@lcc-toulouse.fr*

[e] *Division of Quantum and Physical Chemistry, Celestijnenlaan 200F, Katholieke Universiteit Leuven, B-3001 (Belgium)*

[f] *INPAC – Institute for Nanoscale Physics and Chemistry, Celestijnenlaan 200F, Katholieke Universiteit Leuven, B-3001 (Belgium), Fax: (+) 32 (1632)-7992, E-mail: liviu.chibotaru@chem.kuleuven.be*

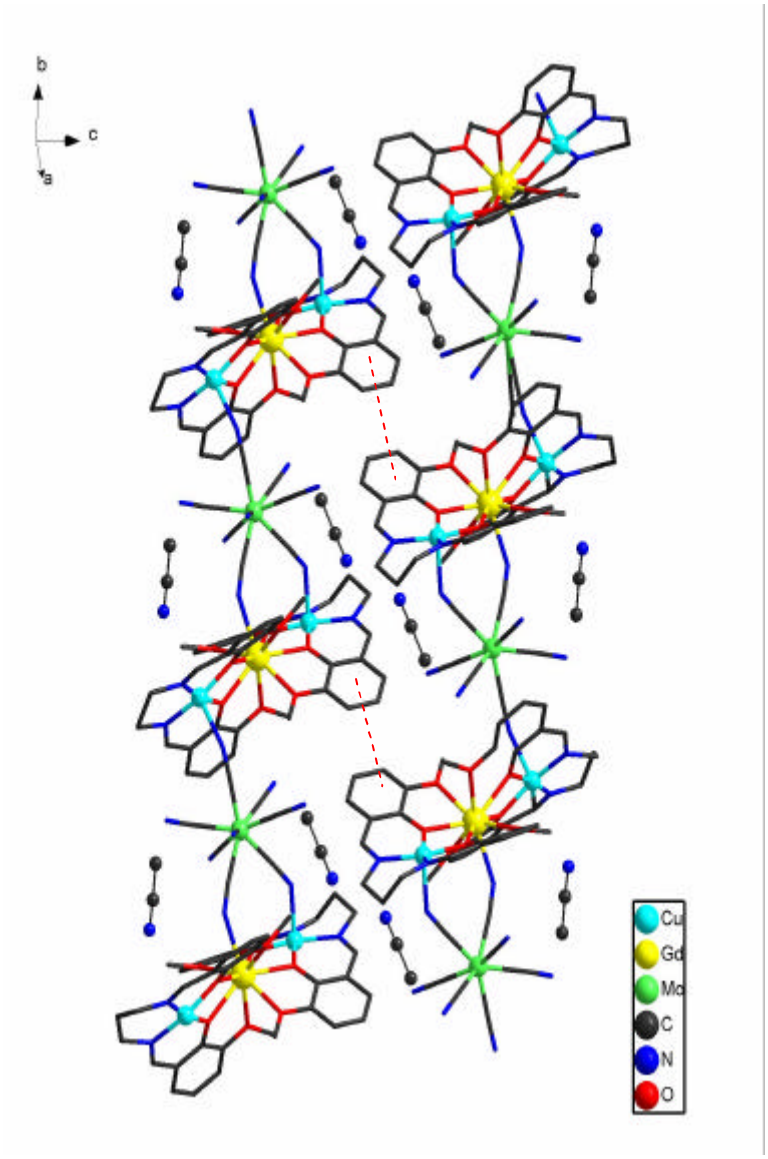

Figure S1. Packing diagram for **1** showing the supramolecular stacking interactions along *b* axis between the phenolic rings (red dotted lines) of the neighbouring chains.

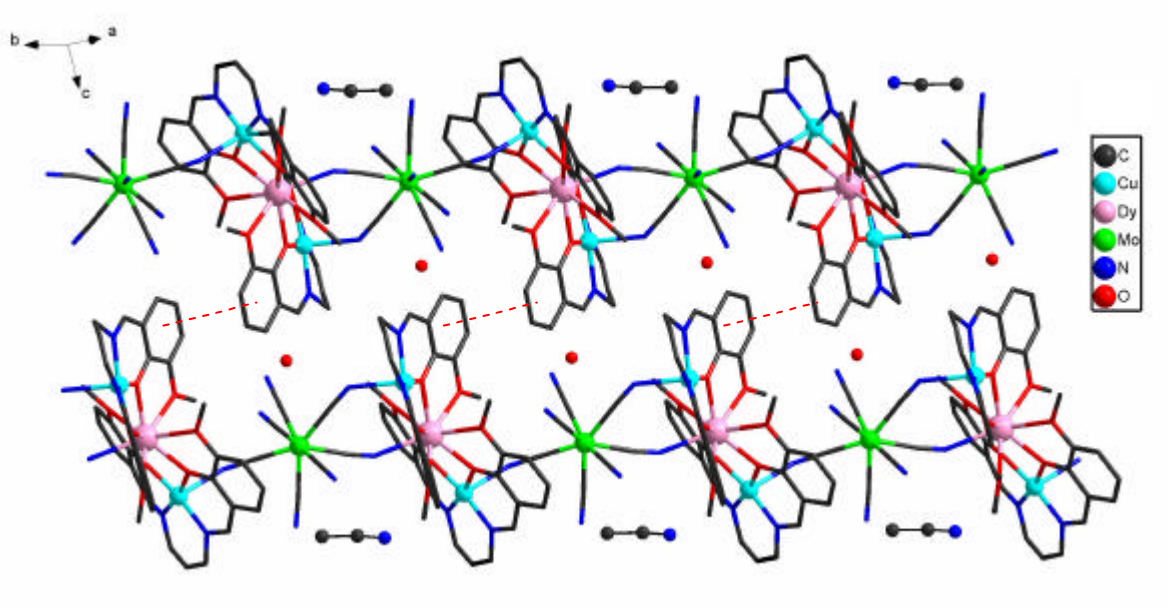

Figure S2. Crystal packing for **2**, showing the weak slipped-off stacking interactions running parallel with *b* axis, between phenolic rings from the neighbouring chains.

Table S1. Results of the SHAPE[1,2] analysis for the {$Mo(CN)_8$} cores in compounds **1** and **2**.

Structure $[M(CN)_8]^{2}$	**(SAPR-8)**[a]	(DD-8)[a]	(JBTP-8)[a]	(SBTP-8)[a]
1	**0.20419**	2.34459	2.69957	23.91355
2	**0.20498**	2.22210	2.63920	23.95293

[a] SAPR-8: *D4d*, Square antiprism; DD-8: *D2d*, Triangular dodecahedron; JBTP-8: *C2*, Biaugmented trigonal prism J50; SBTP-8: *C2v*, Spherical biaugmented trigonal prism.

References

[1] M. Llunell, D. Casanova, J. Cirera, J. M., Bofill, P. Alemany, S. Alvarez, M. Pinsky, D. Avnir, SHAPE: Continuous shape measures of polygonal and polyhedral molecular fragments, 1.1b; University of Barcelona: Barcelona, **2005**.

[2] D. Casanova, M. Llunell, P.Alemany, S. Alvarez *Chem. Eur. J.* **2005,** *11*, 1479-1494.

Ab initio calculation of the magnetic properties of local magnetic centers

Computational Details

Nowadays it is an impossible task to perform a fully ab initio calculation of a infinite chain. Therefore, the chains **1** and **2** in this work have been studied as separate mononuclear metal fragments. In this connection, the question arises to cut suitable mononuclear fragments from the molecule, which would not change significantly the energy structure on the magnetic centre. To have a good description of the 3d or 4f ligand-field states within a fragment one needs to take into account the influence of the neighbouring metal ions. In this respect, the neighbouring Dy^{3+} and Mo^{5+} have been simulated by the closed-shell La^{3+} *ab initio* embedding model potentials (AIMP)[1] and the Cu^{2+} have been simulated by Zn^{2+}-AIMP.[1]

The second approximation concerned the coordination sphere. The structures of the calculated fragments are shown in the Figure S4-S11 below. No geometry optimization on the fragments have been done, all atomic coordinates (except for added hydrogens) being taken from the crystal X-ray analysis. The basis sets used for the calculations were mainly taken from ANO-RCC and ANO-S basis libraries from MOLCAS package.[2]

For the electronic structure, the *ab initio* calculations were performed by means of MOLCAS-7.2 program.[3]

The active space of the complete active space self-consisting field (CASSCF) of calculation of the lanthanides (Dy and Gd) included the 4f orbitals (CAS (9 in 7) for Dy and CAS (7 in 7) for Gd) since we are interested in the ligand field states only. The 4f orbitals are known to be localized, which allows us to consider the charge transfer states much higher in energy, thus being not relevant for the magnetism. The active space of the CASSCF calculation of copper included five 3d orbitals plus another set of five 3d' orbitals to account for the 3d-double shell effect, which is known to be important for the 3d metals with more than 5 electrons in the 3d shell.[4] The active space of the CASSCF calculation of molybdenum included one electron in five 3d orbitals.

The number of roots to be calculates for lanthanides is also a good question. Since the lanthanides have a very strong spin-orbit coupling, a large number of roots should be included in the spin-orbit mixing within the restricted active space state interaction (RASSI-SO) procedure.[5] To exclude all the doubts we calculated all the roots in the active space, but we could mix with spin-orbit interaction only a limited amount of terms. The number and free ion parentage of states mixed by RASSI are listed together with the fragment description below. In the cases of copper and molybdenum we calculated only five doublets coming from ^{2}D multiplet.

The second order multiconfigurational perturbation calculation (CASPT2) was performed only for copper and molybdenum fragments. For lanthanides, due to the multitude of the states needed to be taken into account by spin-orbit coupling, the CASPT2 was too expensive computationally to be done. The CASSCF energies were further used. The spin-orbit coupling was calculated by the RASSI program,[5] but due to some internal limitations of the program itself, and also probably the hardware, it was possible to mix only a limited amount of terms. We took all the roots up to 50000 cm^{-1}. An important aspect of the lanthanide state interaction calculation is one should take into account all the states coming from an entire multiplet. Taking fewer roots than contained in a multiplet may induce strong deviations.

With the obtained spin-orbit multiplets, the powder susceptibility and the g-tensors for the lowest Kramers doublets of isolated fragments were further evaluated using the recently developed *ab initio* methodology.[6] The basis of this approach is to calculate *ab initio* all angular moment matrix elements and then all magnetic moment matrix elements on the relevant spin-orbit multiplets obtained in CASSCF/CASPT2 calculations. These matrix elements are used in a separate routine to calculate:

(i) magnetic properties measured directly in experiment (temperature dependent Van Vleck susceptibility tensor and powder averaged function, field dependent magnetization for different temperatures and directions and the powder magnetization) and

(ii) parameters of magnetic spin Hamiltonians for different spin-orbit multiplets and groups of spin states, described by the corresponding pseudospin, (*g* tensors, zero-field splitting tensors).

In calculations of magnetic properties, all spin-orbit multiplets on the sites are usually taken into account, in particular, all ligand-field states in the case of transition metal ions. This is important for correct quantitative account of the effects of strong magnetic anisotropy and strong applied magnetic fields. Computationally, this routine (single_aniso) was interfaced with MOLCAS-7.2 program.

For the simulation of magnetic properties of polynuclear complexes we used an approach combining the calculated magnetic properties of individual metal fragments (CASSCF/CASPT2/RASSI-SO + single_aniso) with the description of anisotropic exchange interaction between metal sites within the Lines model.[7] The latter begins with the isotropic exchange interactions, which would be in the absence of spin-orbit coupling on metal sites. Diagonalizing the matrix of the corresponding Heisenberg Hamiltonian, written in the basis of spin-orbit multiplets of mononuclear metal fragments, obtained from quantum chemistry calculations, gives solutions corresponding to anisotropic exchange interactions between Kramers doublets of a given metal pair. The main advantage of the Lines model is that it uses one single parameter per metal pair, corresponding to effective isotropic exchange interaction, to simulate the anisotropic exchange coupling. This allows avoiding of overparametrization of the simulations. The exchange model including two structural chain units which have been explicitly taken into account is depicted in the Figure S3. The simulations have been done with a specially designed routine (poly_aniso), which was interfaced with the single_aniso routine treating individual metal fragments.

This *ab initio* based methodology has already been successfully applied for the treatment of the effects of strong magnetic anisotropy in polynuclear transition metal complexes. Thus it allowed to explain the origin of strong anisotropy in dinuclear Co(II) complex of calyx[8]arenes,[8] to rationalize the magnetic data in Co-NC-W pairs of octacyanotungstate(V)-cobalt(II) three-dimensional networks,[9] and to understand the complex magnetism in mixed-valent $Co^{II}_3Co^{III}_4$ heptanuclear wheel, in particular, the lack of SMM behaviour in this compound.[10]

Figure S3. Exchange interactions considered in describing the magnetism of the chains **1** and **2**.

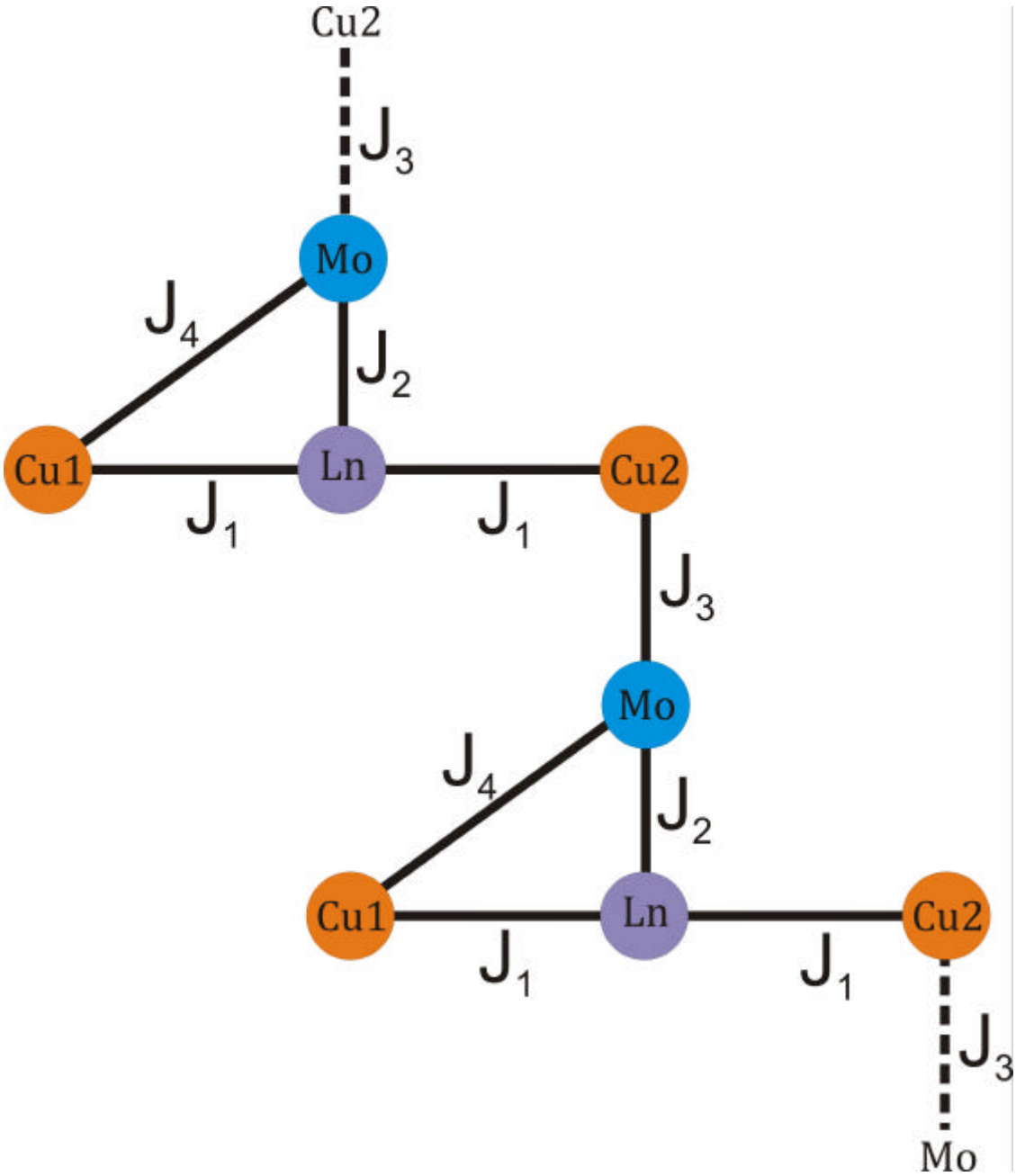

CASSCF / CASPT2 calculations for metal fragments of crystal 1

Fragment Gd^{3+}

Figure S4. The structure of the calculated fragment of the Gd^{3+}.

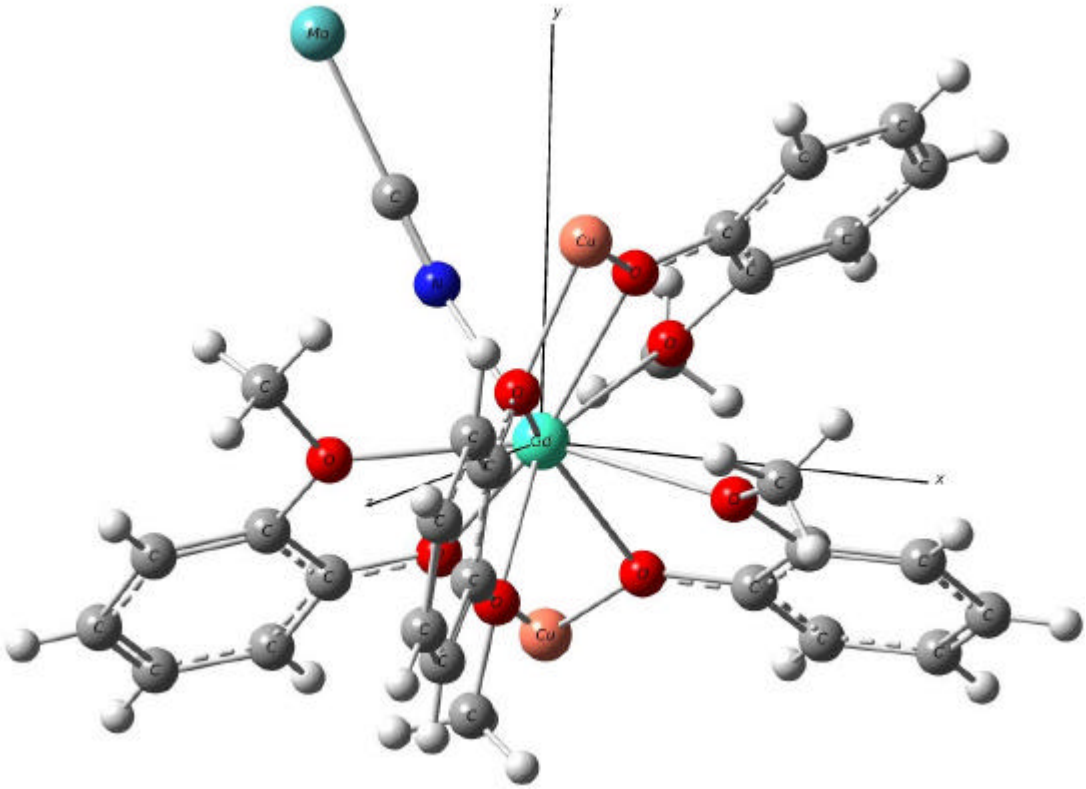

Basis Sets

ANO-RCC [8s7p5d4f2g1h] – for Gd^{3+}.

ANO-RCC [3s2p1d] – for O and N.

ANO-S [3s2p1d] – for C.

ANO-S [2s1p] – for H.

ECP---La.ECP.deGraaf.0s.0s.0e-La(LaMnO3). – for Mo^{5+}.

ECP---Zn.ECP.Lopez-Moraza.0s.0s.0e-AIMP-KZnF3. – for Cu^{2+}.

Active space:

CAS(7 in 7).

Calculated roots:

All the states coming from the following multiplets have ben taken into account in the spin-orbit interaction (RASSI):

^{8}S (the only one existing octet), ^{6}I, ^{6}H, ^{6}G, ^{6}F, ^{6}D, ^{6}P (all sextets), ^{4}D, ^{4}N, ^{4}H, ^{4}L, ^{4}K, ^{4}F, ^{4}G, ^{4}H, ^{4}G, ^{4}S, ^{4}I, ^{4}I, ^{4}D, ^{4}M, ^{4}K (171 out of 392 quartets), ^{2}Q, ^{2}G, ^{2}F, ^{2}M, ^{2}L, ^{2}O, ^{2}I (113 out of 792 doublets).

Table S2. Lowest calculated terms and Kramers doublets on Gd^{3+} fragment.

Spin Multiplicity		CASSCF (cm^{-1})	Kramers doublets (cm^{-1})
1	8	0.000	0.000 0.361 0.629 1.020
1	6	40869.576	39538.884
2	6	40887.910	39589.684
3	6	40904.864	39627.063
4	6	43661.718	39676.455
5	6	43662.199	40074.208
…	…	…	40104.021
1	4	43670.287	40141.363
2	4	43676.714	40629.482
3	4	43681.515	40670.410
4	4	43689.798	43071.919
5	4	43693.638	43084.368
…	…	…	43109.070
1	2	43709.390	43162.441
2	2	43721.039	43410.671
3	2	43745.289	43422.517
4	2	43794.157	43439.926
5	2	48936.267	43464.821
…	…	…	43496.280

Table S3. The g-tensor of the ground state of Gd^{3+} in the basis of $\tilde{S} = 7/2$

	Spin-Orbit energy (cm^{-1})	g tensor of the ground $\tilde{S} = 7/2$	Magnetic Axes		
1	0.000	g_x=1.996186	0.9245	0.3794	-0.0351
		g_y=1.996190	-0.1150	0.1898	-0.9750
		g_z=1.996207	-0.3633	0.9055	0.2191

Figure S5. The structure of the calculated fragment of the $Cu1^{2+}$.

Fragment $Cu1^{2+}$

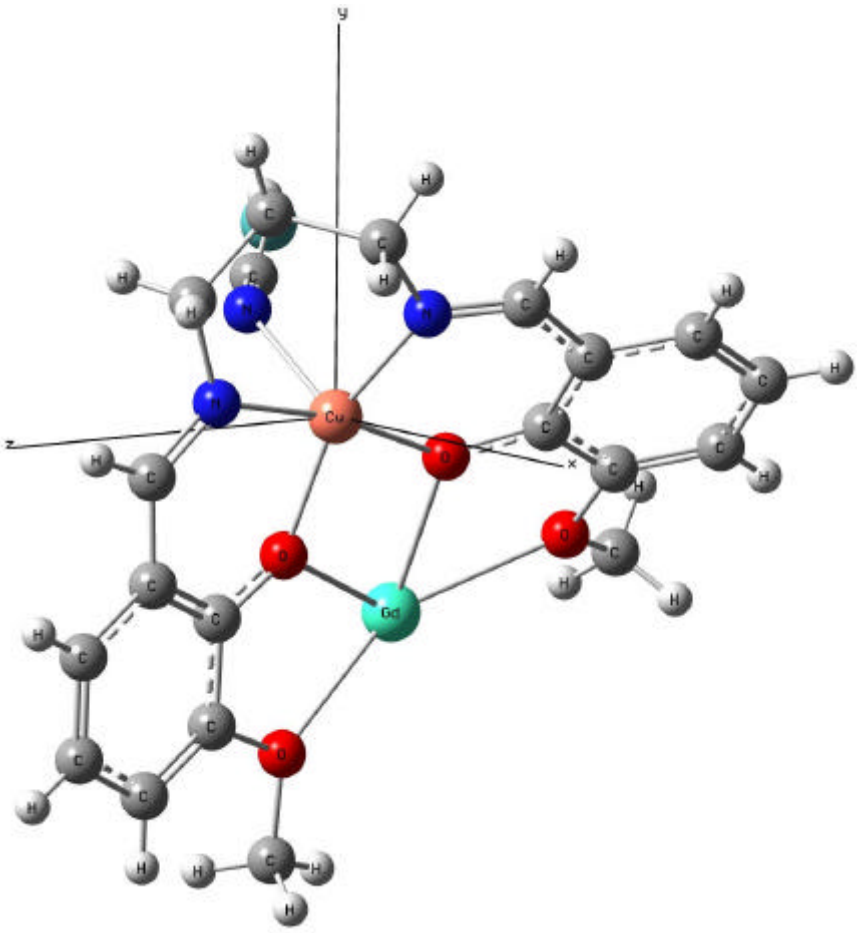

Basis Sets

ANO-RCC [6s5p3d2f1g] – for Cu^{2+}.

ANO-RCC [3s2p1d] – for O and N.

ANO-S [3s2p1d] – for C.

ANO-S [2s1p] – for H.

ECP---La.ECP.deGraaf.0s.0s.0e-La(LaMnO3). – for Mo^{5+} and Gd^{3+}.

Active space:

CAS(9 in 5+5) including the 3d-double shell effect.

Calculated roots:

All the states coming from ^{2}D multiplet.

Table S4. Lowest calculated terms and Kramers doublets on $Cu1^{2+}$ fragment.

	Spin Multiplicity	CASSCF / CASPT2 (cm^{-1})	Kramers doublets (cm^{-1})
1	2	0.000	0.000
2	2	15443.412	15140.873
3	2	16212.831	16017.958
4	2	17074.024	17181.526
5	2	17676.991	18359.392

Table S5. The g-tensor of the ground Kramers doublet of $Cu1^{2+}$.

	Spin-Orbit energy (cm^{-1})	g tensor of the ground $\tilde{S} = 1/2$	Magnetic Axes		
1	0.000	g_x= 2.065506	0.1338	0.3910	0.9106
		g_y= 2.090601	0.4880	0.7737	-0.4039
		g_z= 2.358383	-0.8625	0.4985	-0.0873

Figure S6. The structure of the calculated fragment of the $Cu2^{2+}$.

Fragment $Cu2^{2+}$

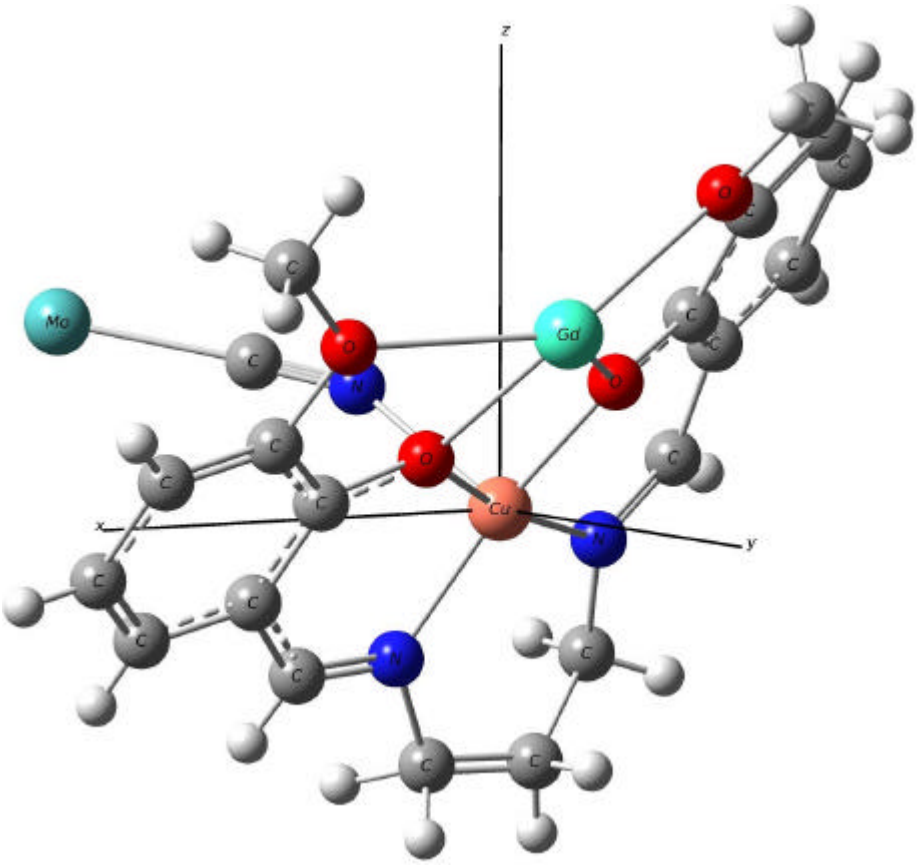

Basis Sets

ANO-RCC [6s5p3d2f1g] – for Cu^{2+}.

ANO-RCC [3s2p1d] – for O and N.

ANO-S [3s2p1d] – for C.

ANO-S [2s1p] – for H.

ECP---La.ECP.deGraaf.0s.0s.0e-La(LaMnO3). – for Mo^{5+} and Gd^{3+}.

Active space:

CAS(9 in 5+5) including the 3d-double shell effect.

Calculated roots:

All the states coming from ^{2}D multiplet.

Table S6. Lowest calculated terms and Kramers doublets on $Cu2^{2+}$ fragment.

	Spin Multiplicity	CASSCF / CASPT2 (cm^{-1})	Kramers doublets (cm^{-1})
1	2	0.000	0.000
2	2	16173.010	15794.380
3	2	16272.593	16043.043
4	2	17262.037	17455.297
5	2	17828.087	18531.489

Table S7. The g-tensor of the ground Kramers doublet of $Cu2^{2+}$.

	Spin-Orbit energy (cm^{-1})	g tensor of the ground $\tilde{S} = 1/2$	Magnetic Axes		
1	0.000	g_x= 2.060806	0.8759	0.4029	0.2655
		g_y= 2.079046	-0.4284	0.3962	0.8121
		g_z= 2.319866	0.2220	-0.8251	0.5196

Figure S7. The structure of the calculated fragment of the Mo^{5+}.

Fragment Mo^{5+}

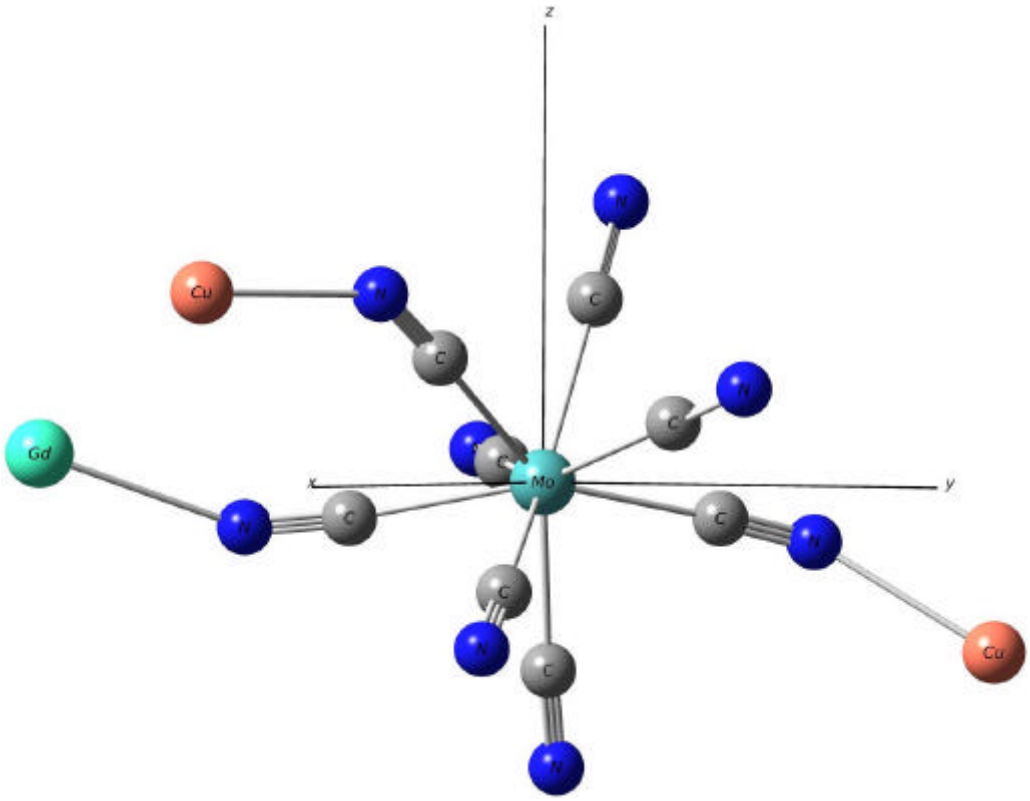

Basis Sets

ANO-RCC [7s6p4d2f1g] – for Mo^{5+}.

ANO-RCC [3s2p1d] – for C and N.

ECP --- La.ECP.deGraaf.0s.0s.0e-La(LaMnO3). – for Gd^{3+}.

ECP --- Zn.ECP.Lopez-Moraza.0s.0s.0e-AIMP-KZnF3 – for Cu^{2+}.

Active space:

CAS(1 in 5).

Calculated roots:

All the states coming from ^{2}D multiplet.

Table S8. Lowest calculated terms and Kramers doublets on Mo^{5+} fragment.

	Spin Multiplicity	CASSCF / CASPT2 (cm^{-1})	Kramers doublets (cm^{-1})
1	2	0.000	0.000
2	2	33109.729	33036.011
3	2	37849.900	37922.985
4	2	43891.696	43882.114
5	2	47783.764	47865.436

Table S9. The g-tensor of the ground Kramers doublet of Mo^{5+}.

	Spin-Orbit energy (cm^{-1})	g tensor of the ground $\tilde{S} = 1/2$	Magnetic Axes		
1	0.000	g_x= 1.946568	-0.5979	-0.5502	-0.5829
		g_y= 1.953939	-0.8013	0.4301	0.4159
		g_z= 2.001517	-0.0219	-0.7157	0.6980

CASSCF / CASPT2 calculations for metal fragments of crystal 2

Figure S8. The structure of the calculated fragment of the Dy^{3+}.

Fragment Dy^{3+}

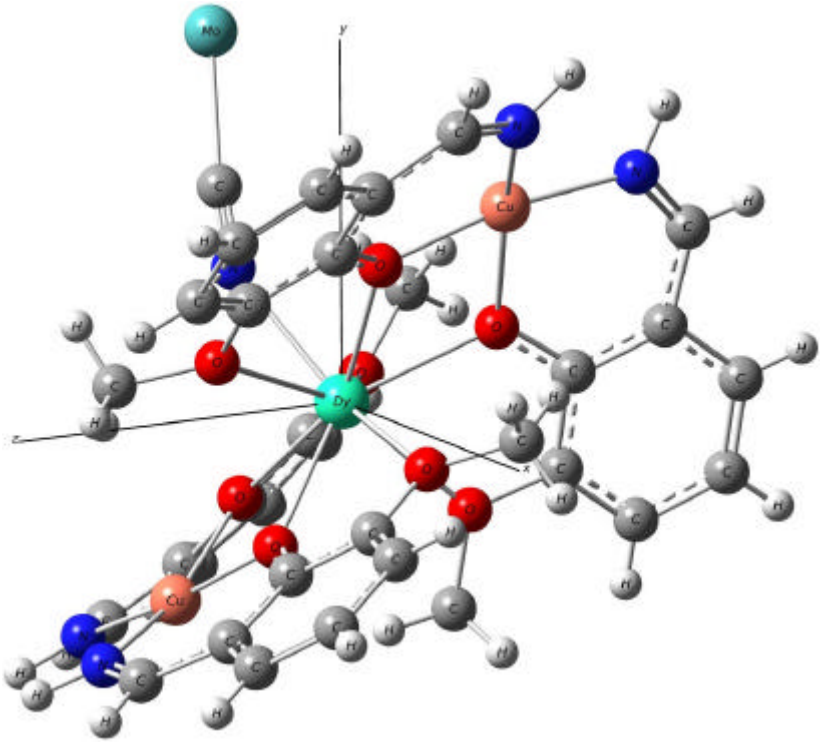

Basis Sets

ANO-RCC [8s7p5d4f2g1h] – for Dy^{3+}.

ANO-RCC [3s2p1d] – for O and N.

ANO-S [3s2p1d] – for C.

ANO-S [2s1p] – for H.

ECP---La.ECP.deGraaf.0s.0s.0e-La(LaMnO3). – for Mo^{5+}.

ECP---Zn.ECP.Lopez-Moraza.0s.0s.0e-AIMP-KZnF3. – for Cu^{2+}.

Active space:

CAS(9 in 7).

Calculated roots:

All the states coming from the following multiplets have been taken into account in the spin-orbit interaction (RASSI):

^{6}H, ^{6}F, ^{6}P (all sextets), ^{4}I, ^{4}F, ^{4}M, ^{4}G, ^{4}L, ^{4}D, ^{4}H, ^{4}P, ^{4}G, ^{4}F, ^{4}I (128 out of 224 quartets), ^{2}L, ^{2}K, ^{2}P, ^{2}N, ^{2}F, ^{2}M, ^{2}H, ^{2}D, ^{2}G, ^{2}O (130 out of 490 doublets).

Table S10. Lowest calculated terms and Kramers doublets on Dy^{3+} fragment.

	Spin Multiplicity	CASSCF (cm^{-1})	Kramers doublets (cm^{-1})
1	6	0.000	0.000
2	6	19.361	141.263
3	6	170.629	237.381
4	6	218.360	305.529
5	6	307.120	389.704
6	6	318.478	439.891
7	6	508.586	478.360
8	6	570.138	558.680
9	6	575.371	3622.502
10	6	611.895	3718.451
11	6	672.907	3822.158
12	6	7635.080	3849.708
13	6	7789.857	3907.123
14	6	7834.123	3980.584
15	6	7847.048	4032.079
16	6	7867.992	6211.163
17	6	7897.681	6279.714
18	6	7912.579	6363.401
19	6	34812.636	6398.790
20	6	35143.282	6490.199
21	6	35454.487	6556.954
1	4	24909.772	8189.734
2	4	24911.202	8245.033
3	4	25012.162	8307.342
4	4	25018.136	8415.851
5	4	25024.184	8494.132
…	…	…	9729.385
1	2	37394.124	9792.946
2	2	37396.231	9867.740
3	2	37449.487	10043.444
4	2	37473.595	10133.572
5	2	37499.111	10187.832
…	…	…	…

Table S11. The g-tensor of the ground Kramers doublet of Dy^{3+}.

	Spin-Orbit energy (cm^{-1})	g tensor of the ground KD	Magnetic Axes		
1	0.000	g_x=0.023670	0.6567	-0.6414	-0.3966
		g_y=0.043737	0.6042	0.1329	0.7856
		g_z=19.582441	-0.4512	-0.7556	0.4749

Figure S9. The structure of the calculated fragment of the $Cu1^{2+}$.

Fragment $Cu1^{2+}$

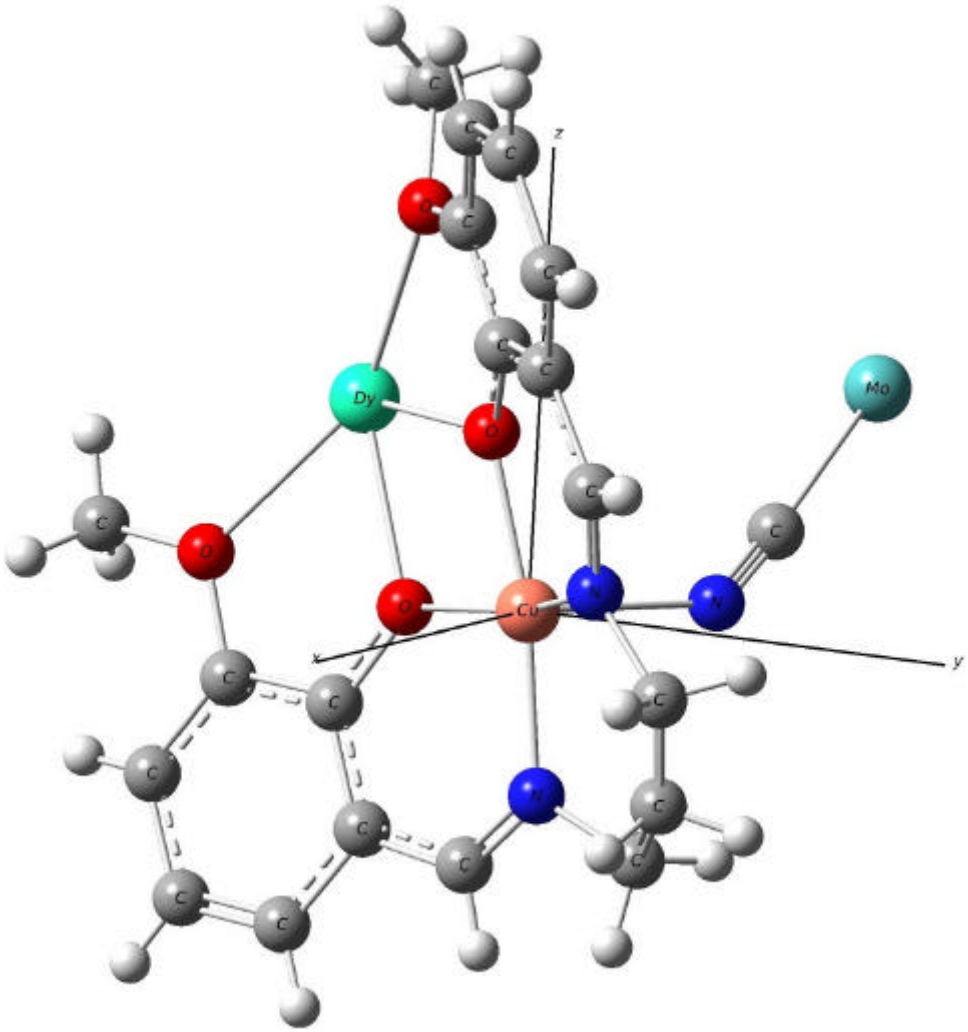

Basis Sets

ANO-RCC [6s5p3d2f1g] – for Cu^{2+}.

ANO-RCC [3s2p1d] – for O and N.

ANO-S [3s2p1d] – for C.

ANO-S [2s1p] – for H.

ECP---La.ECP.deGraaf.0s.0s.0e-La(LaMnO3). – for Mo^{5+} and Gd^{3}

Active space:

CAS(9 in 5+5) including the 3d-double shell effect.

Calculated roots:

All the states coming from ^{2}D multiplet.

Table S12. Lowest calculated terms and Kramers doublets on $Cu1^{2+}$ fragment.

	Spin Multiplicity	CASSCF / CASPT2 (cm^{-1})	Kramers doublets (cm^{-1})
1	2	0.000	0.000
2	2	15504.000	15235.096
3	2	16492.592	16235.039
4	2	17104.644	17233.402
5	2	17825.771	18514.767

Table S13. The g-tensor of the ground Kramers doublet of $Cu1^{2+}$.

	Spin-Orbit energy (cm^{-1})	g tensor of the ground $\tilde{S} = 1/2$	Magnetic Axes		
1	0.000	g_x= 2.062837	-0.0639	-0.2005	0.9776
		g_y= 2.079367	0.5284	0.8242	0.2036
		g_z= 2.328436	-0.8466	0.5296	0.0533

Figure S10. The structure of the calculated fragment of the $Cu2^{2+}$.

Fragment $Cu2^{2+}$

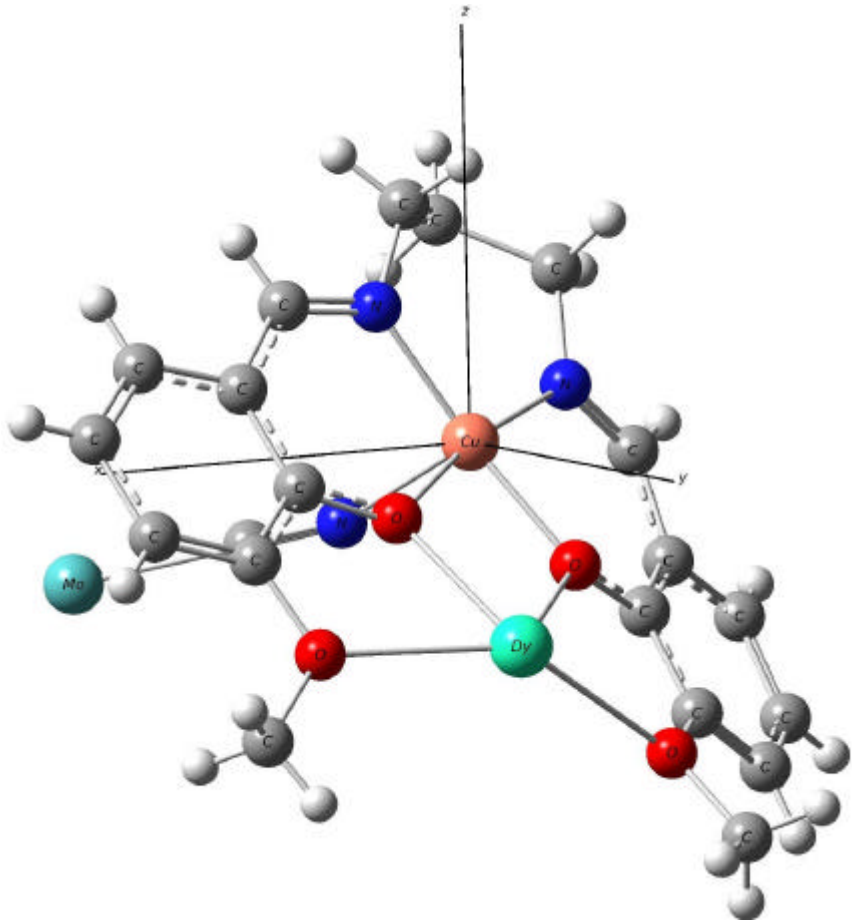

Basis Sets

ANO-RCC [6s5p3d2f1g] – for Cu^{2+}.

ANO-RCC [3s2p1d] – for O and N.

ANO-S [3s2p1d] – for C.

ANO-S [2s1p] – for H.

ECP---La.ECP.deGraaf.0s.0s.0e-La(LaMnO3). – for Mo^{5+} and Gd^{3+}.

Active space:

CAS(9 in 5+5) including the 3d-double shell effect.

Calculated roots:

All the states coming from ^{2}D multiplet

Table S14. Lowest calculated terms and Kramers doublets on $Cu2^{2+}$ fragment.

	Spin Multiplicity	CASSCF / CASPT2 (cm^{-1})	Kramers doublets (cm^{-1})
1	2	0.000	0.000
2	2	16447.194	16141.011
3	2	16767.889	16422.603
4	2	17500.164	17691.166
5	2	18097.067	18841.271

Table S15. The g-tensor of the ground Kramers doublet of $Cu2^{2+}$.

	Spin-Orbit energy (cm^{-1})	g tensor of the ground $\tilde{S} = 1/2$	Magnetic Axes		
1	0.000	g_x= 2.063452	-0.7224	-0.4857	0.4921
		g_y= 2.084169	0.6576	-0.2627	0.7061
		g_z= 2.347225	-0.2137	0.8337	0.5092

Figure S11. The structure of the calculated fragment of the Mo^{5+}

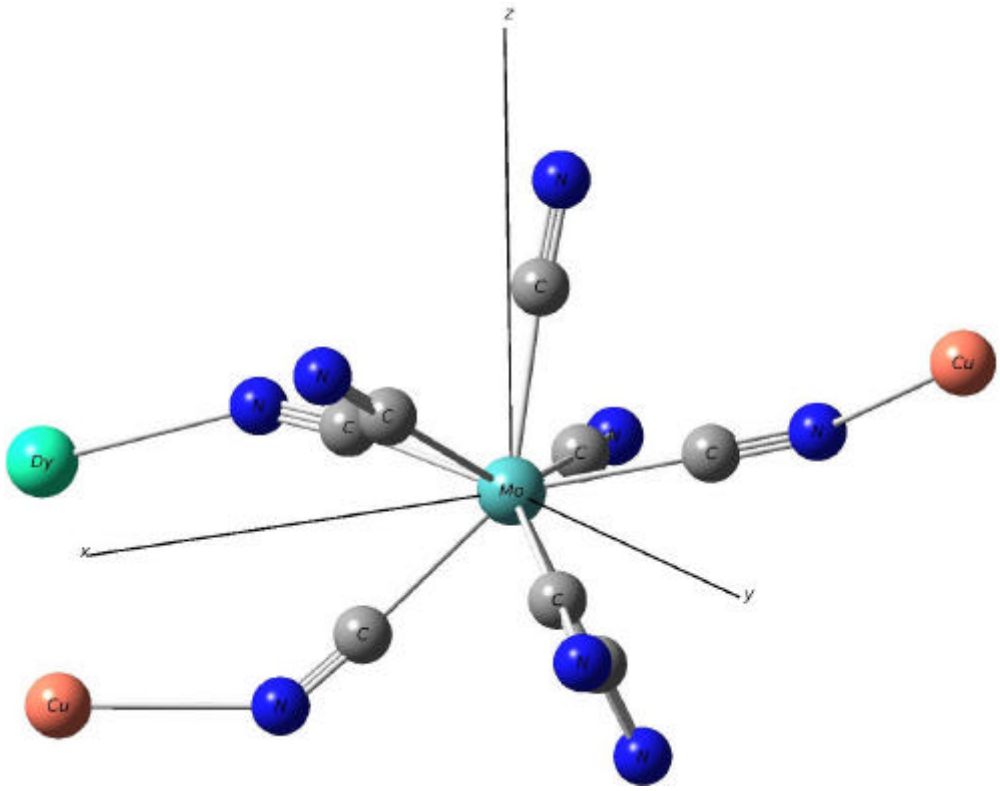

Basis Sets

ANO-RCC [7s6p4d2f1g] – for Mo^{5+}.

ANO-RCC [3s2p1d] – for C and N.

ECP --- La.ECP.deGraaf.0s.0s.0e-La(LaMnO3). – for Gd^{3+}.

ECP --- Zn.ECP.Lopez-Moraza.0s.0s.0e-AIMP-KZnF3 – for Cu^{2+}.$^{+}$.

Active space:

CAS(1 in 5).

Calculated roots:

All the states coming from ^{2}D multiplet.

Table S16. Lowest calculated terms and Kramers doublets on Mo^{5+} fragment.

	Spin Multiplicity	CASSCF / CASPT2 (cm^{-1})	Kramers doublets (cm^{-1})
1	2	0.000	0.000
2	2	33409.395	33334.014
3	2	37980.168	38056.980
4	2	44007.156	44002.269
5	2	48647.477	48720.940

Table S17. The g-tensor of the ground Kramers doublet of Mo^{5+}.

	Spin-Orbit energy (cm^{-1})	g tensor of the ground $\tilde{S} = 1/2$	Magnetic Axes		
1	0.000	g_x= 1.952573	0.1876	0.6075	-0.7718
		g_y= 1.957119	0.9809	-0.1569	0.1150
		g_z= 2.001122	0.0512	0.7787	0.6253

DFT Calculations of the exchange couplings of Mo-Cu1 and Mo-Cu2 pairs

In order to start with some approximate value of the exchange parameters in the fully ab initio model (Figure S3) we performed broken symmetry DFT calculation of the Mo-Cu1 and Mo-Cu2 pairs from the MoCu2Dy chain.

The DFT calculations were done with the ADF program package.

The basis sets were taken from the TZP and DZ basis libraries from ADF. The metal ions and the atoms from the first coordination had TZP basis while the distant atoms were taken into account with DZ basis. The B3Lyp functional was used for all calculations.

Both calculated structures are quite similar. The figure S12 shows the calculated structure of the fragment Mo-Cu1.

Figure S12. The structure of the calculated fragment of Mo-Cu1.

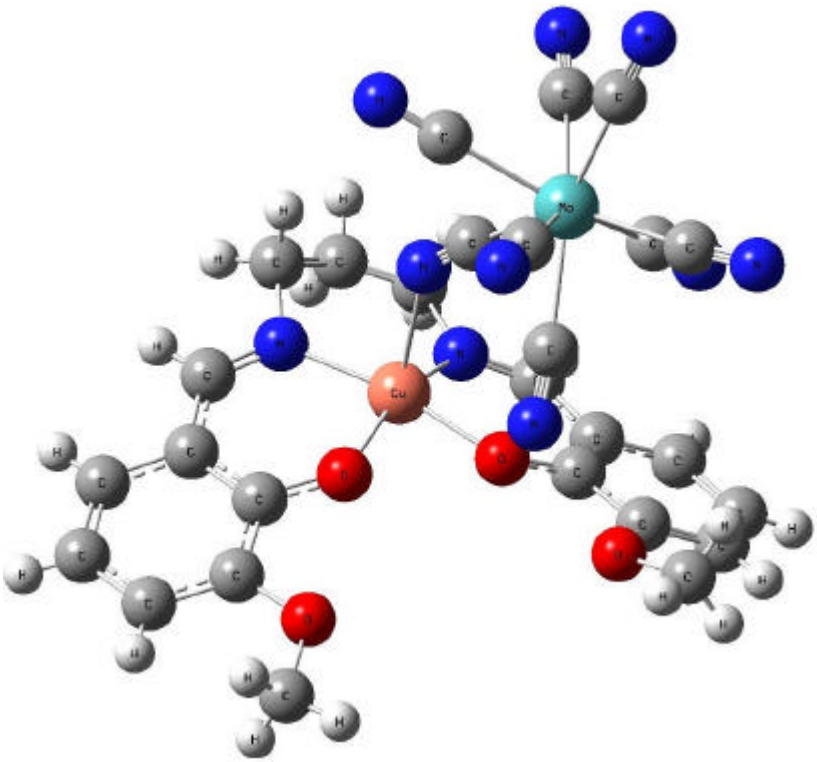

Table S18. Energies of the calculated configurations (cm^{-1}).

	Mo-Cu1	Mo-Cu2
$Mo^{\uparrow} - Cu^{\uparrow}$	0.0	0.0
$Mo^{\uparrow} - Cu^{\downarrow}$	1.6	5.2

Figure S13. Magnetic molecular orbitals (containing unpaired electrons) of the Mo-Cu1 fragment.

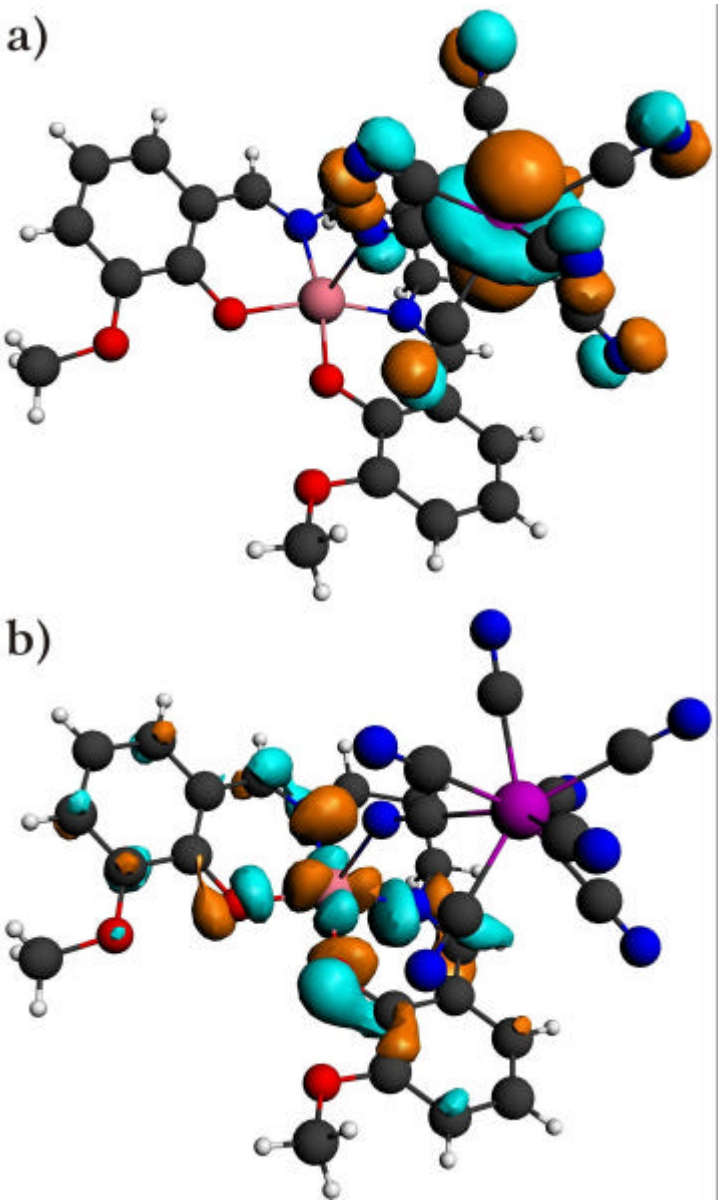

References

[1] L. Seijo, Z. Barandiarán in *Computational Chemistry: Reviews of Current Trends, 4* (Ed. by J. Leszcynski), **1999**, World Scientific, Singapur, pp. 55-152.

[2] K. Pierloot, B. Dumez, P.-O. Widmark and B. O. Roos, *Theor. Chim. Acta* **1995**, *90*, 87; B. O. Roos, R. Lindh, P-O. Malmqvist,V. Veryazov V., P. O. Widmark, *J. Phys. Chem. A* **2004**, *108*, 2851.

[3] G. Karlström, R. Lindh, P. -Å. Malmqvist, B. O. Roos, U. Ryde, V. Veryazov, P. -O. Widmark, M. Cossi, B. Schimmelpfennig, P. Neogrady, L. Seijo, *Comp. Mater. Sci.* **2003**, *28*, 222-239.

[4] K. Andersson, B. O. Roos, *J. Chem. Phys. Lett.* **1992**, *191*, 507-514.

[5] B. O. Roos, P-O. Malmqvist, *Phys. Chem. Chem. Phys.* **2004**, *6*, 2919.

[6] L. F. Chibotaru, L. Ungur, Program SINGLE_ANISO, University of Leuven **2006**.

[7] M. E. Lines, *J. Chem. Phys.* **1971**, *55*, 2977-2984.

[8] S. Petit, G. Pillet, D. Luneau, L.F. Chibotaru, L. Ungur, *Dalton Trans.* **2007**, 4582-4588.

[9] S. Clima, M. F. A. Hendrickx, L. F. Chibotaru, A. Soncini, V. S. Mironov, A. Ceulemans, *Inorg. Chem.* **2007**, *46*, 2682-2690.

[10] L. F. Chibotaru, L. Ungur, Ch. Aronica, H. Elmoll, G. Pilet, D. Luneau, *J. Am. Chem. Soc.* **2008**, *130* (37), 12445-12455.

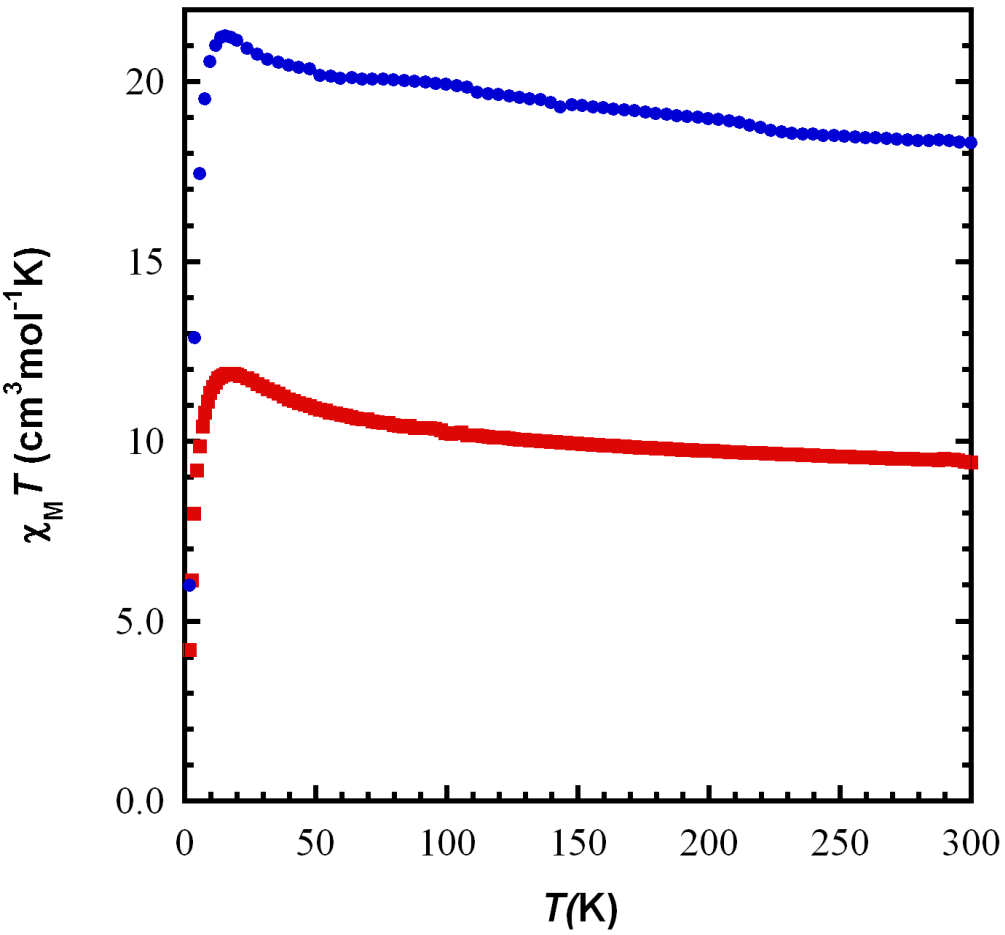

Figure S14. Plot of χ_MT vs. T for compound **4** and **5**.

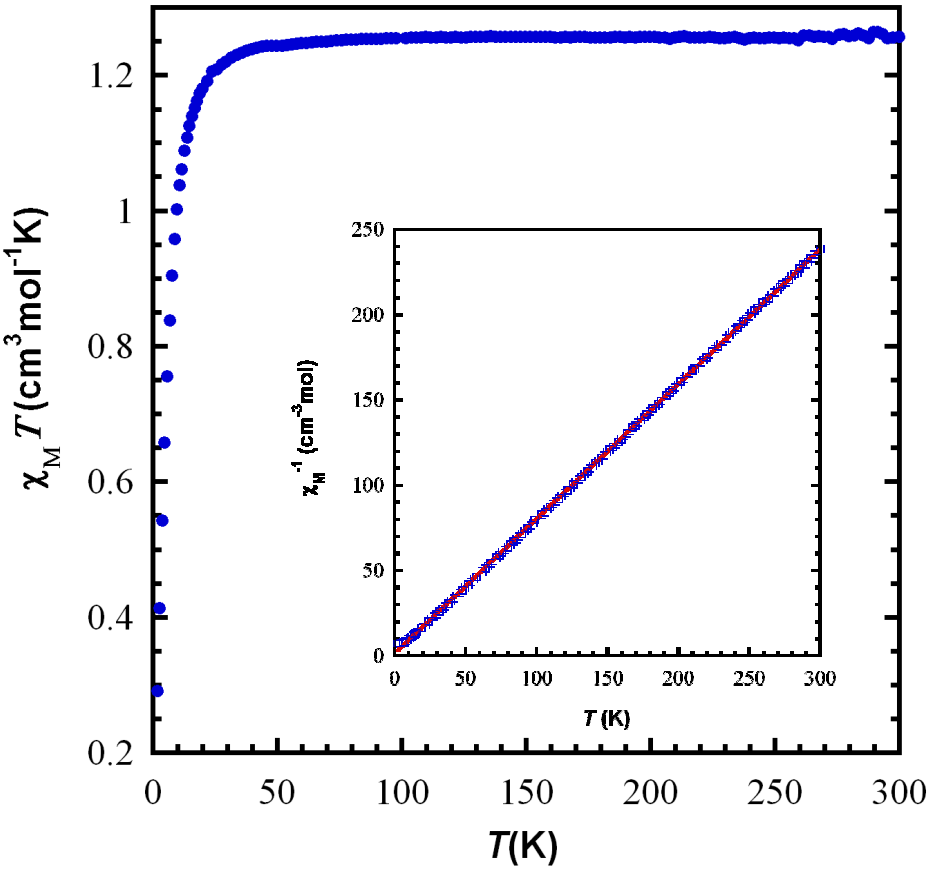

Figure S15. Plot of $\chi_M T$ vs. T for compound **3** (the inset shows plot of $1/\chi_M$ vs. T; the solid line presents the best theoretical fit).

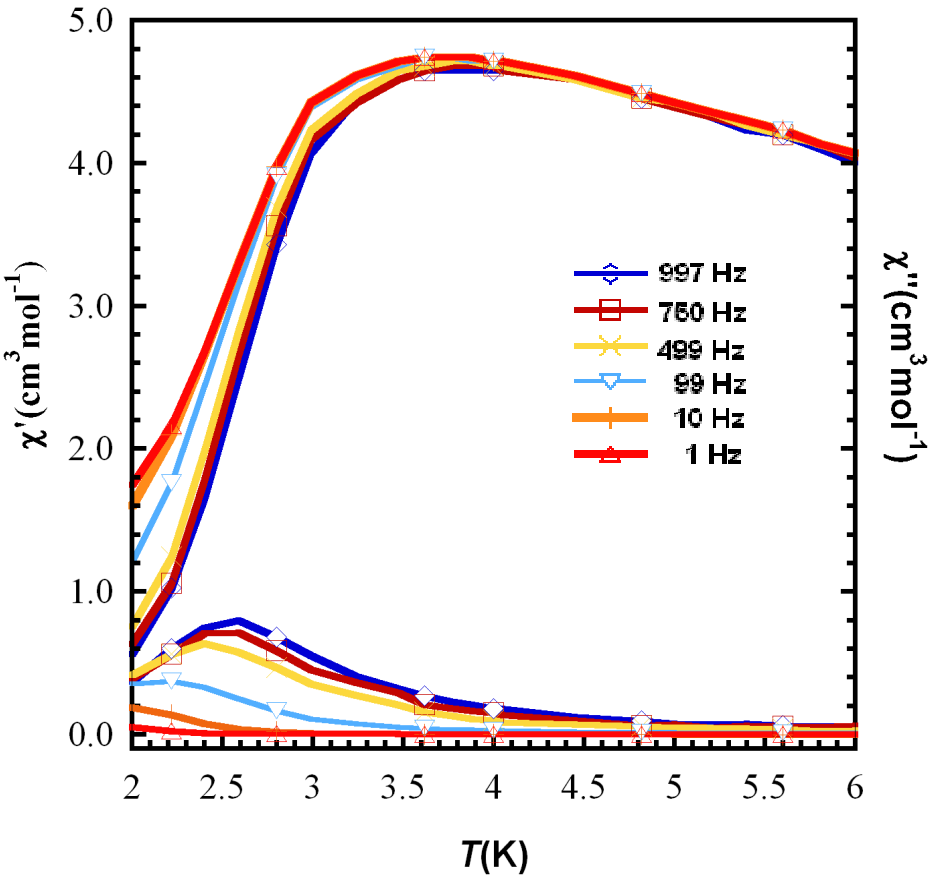

Figure S16. Plots of the in-phase (c_M') signal (top) vs T and out-of-phase (c_M'') signal (bottom) vs T in ac magnetic susceptibility at different frequencies for **5**.

Table S19. Crystal data and structure refinement for compounds **3** and **5**

	3	**5**
Empirical formula	$C_{46}H_{40}N_{12}O_{10}Cu_2LaW$	$C_{56}H_{55}N_{17}O_8Cu_2DyW$
Formula weight	1370.74	1567.60
Temperature	293(2) K	180 K
Wavelength	0.71073 Å	0.71073 Å
Crystal system, space group	Triclinic, *P-1*	Triclinic, *P-1*
Unit cell dimensions	a = 11.4580(5) Å b = 12.4306(6) Å c = 20.5668(11) Å a = 94.891(4)° b = 101.823(4)° g = 116.255(3)°	a = 12.4449(4) Å b =13.8659(6) Å c = 18.1553(8) Å a =100.333(3)° b = 97.008(2)° γ = 95.089(2)°
Volume	2519.2(2) Å^3	3039.4(2) Å^3
Z	2	2
Calculated density (g/cm^3)	1.807	1.713
Absorbtion coefficient	4.007 mm^{-1}	3.858 mm^{-1}
F(000)	1338	1544
Crystal size	0.05×0.1×0.2	0.03×0.12×0.15 mm
Theta range for data collection	2.31 to 33.47	3 to 25°
Limiting indices	$-17 \le h \le 17$, $-19 \le k \le 19$, $-31 \le l \le 31$	$-16 \le h \le 16$, $-18 \le k \le 18$, $-24 \le l \le 24$
Reflecting collected/unique	47883 / 19052 [R_{int} = 0.0645]	54991 / 11861 [R_{int} = 0.045]
Max. and min. transmission	0.7123 and 0.4476	0.89 and 0.55
Data/restraints/parameters	19052/0/658	9120/0/738
Goodness-of-fit on F^2	1.003	1.1109
Final R indices	$R1$ = 0.0593, $wR2$ = 0.1042 [$I > 2s(I)$]	$R1$ = 0.0313, $wR2$ = 0.0354 [$I > 3\ s(I)$]
R indices (all data)	$R1$ = 0.1166, $wR2$ = 0.1207	$R1$ = 0.0644, $wR2$ = 0.0511